Theranostic Lysosomal Targeting Anticancer and Antimetastatic Agents: Half-sandwich Iridium (III) Rhodamine complexes

Wenli Ma[†], Xingxing Ge[†], Zhishan Xu[†‡], Shumiao Zhang[†], Xiangdong He†, JuanJuan Li†, Xiaorong Xia[†], Xiaobing Chen[†], Zhe Liu*[†]

†Institute of Anticancer Agents Development and Theranostic Application, The Key Laboratory of Life-Organic Analysis and Key Laboratory of Pharmaceutical Intermediates and Analysis of Natural Medicine, Department of Chemistry and Chemical Engineering, Qufu Normal University, Qufu 273165, China.

‡Department of Chemistry and Chemical Engineering, Shandong Normal University, Jinan 250014, China

*Corresponding author. Email: liuzheqd@163.com

EXPERIMENTAL SECTION

Experimental Section

UV-Vis Spectroscopy

The UV-Vis spectra of the compounds were recorded by TU-1901 UV spectrophotometer with 1 cm path-length quartz cuvettes (3 mL). Spectra were processed using UV-inlab software. Experiments were carried out at 298 K unless otherwise stated.

The stability and fluorescence characteristics of complexes

The stability of the complexes in solution was investigated. Taking complex **2** as example, a 20 μM concentration of the complex solution was prepared in PBS buffer solution（pH = 7.4）and monitored by the UV-Vis spectroscopy over 24 h at 298 K. The stability results of the complexes are shown in Figure S1. As the time went by, the absorption peaks of the complex did not change significantly, indicating that the structures of complex **2** was stable. The fluorescence characteristics of the complex is also detected by a fluorescence spectrophotometer (Figure 1). The complex has very good fluorescence characteristics in vitro and the complex structure is stable. The stability and fluorescence properties of the complex structure provide the basis for subsequent cell experiments.

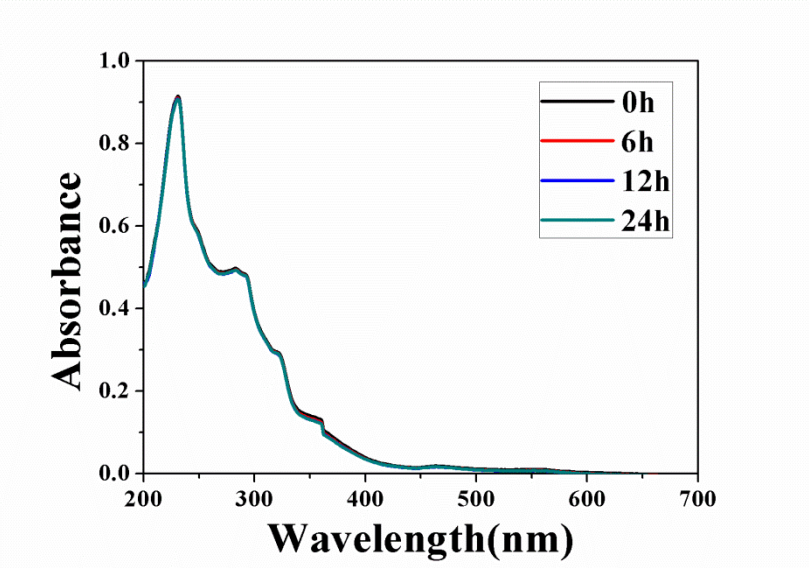

Figure S1. UV-Vis absorption spectra of complex **2** (20 μM) in PBS buffer during incubation at 298 K.

BSA binding studies

In order to study the transport of complexes into the human body. Taking the interaction between complex **1** and BSA as an example (Figure 2). In order to counteract the self-absorption of complex **1** in the ultraviolet range, we studied the UV-visible absorption spectrum of BSA (10 μM).[1-3] The sample cell and the reference ratio were compared. In the cuvette, a uniform concentration gradient of the iridium complex (0.4 μM) was added. The UV absorption spectrum shows that absorption peaks significantly decreased and red shifted at 218 nm. This dramatic decrease can be attributed to the induced perturbation of the α-helix of BSA by the complexes and the obvious red-shift in the absorption spectra is due to the effect of the polar solvent (water). In addition, the increase in the absorption peak of BSA at 278 nm was observed and there was no red-shift or blue-shift phenomenon, indicating that the iridium complexes may interact with the three aromatic compounds (Trp, Tyr and Phe) in the BSA microenvironment.[4, 5]

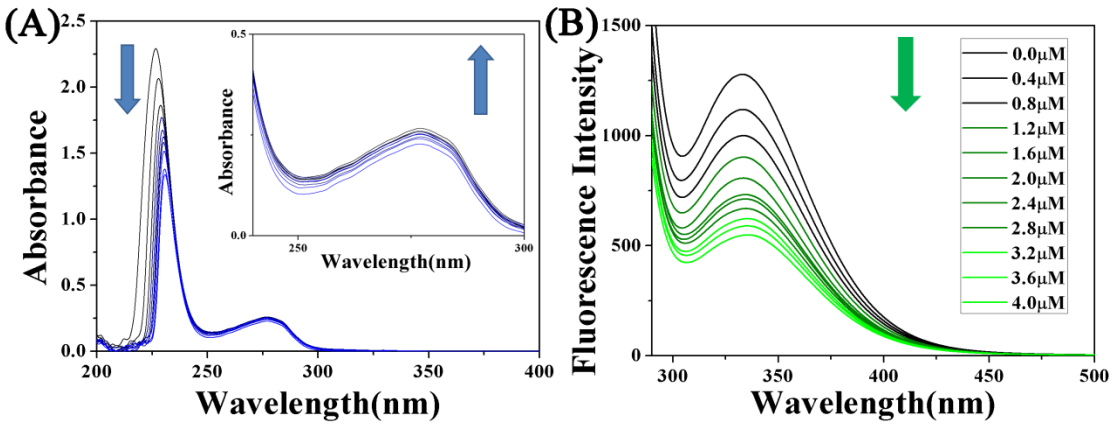

Figure S2. (A) UV-Vis spectra of BSA (10 μM, 50 mM Tris-HCl, 50 mM NaCl, pH = 7.2) and complex **2** (0~4.0 μM) reaction. Arrows indicate the direction of change in absorbance. Inset: UV absorption spectra from 240 nm to 300 nm (B) Fluorescence spectra of BSA (10 μM, 50 mM Tris-HCl, 50 mM NaCl, pH = 7.2) reacted with complex **2** (0~4.0 μM) (BSA:10 μM; λex= 280 nm; λem= 343 nm).

Second, we use fluorescence spectrophotometers to further study the interactions between iridium complexes and BSA. This work was calibrated during the fluorescence measurement to correct for the effect of the "internal filter". Fluorescence spectra of the addition of iridium complex (0.4 μM) in a concentration gradient in the presence of BSA (10 μM) are shown in Figure 5.The fluorescence quenching mechanism has been previously reported to be classified into static quenching and dynamic quenching. The fluorescence intensity of BSA at 343 nm decreases with the increase of the concentration of complex **1**, indicating that the interaction between BSA and the complex is a static quenching mode (Figure S4).[6, 7] Possible quenching mechanisms can be expressed using the Stern-Volmer equation (Equ 1).

$$F_0/F = 1 + K_{SV}[Q] = 1 + K_q\tau_0 \qquad (1)$$

Where F_0 and F are expressed as the fluorescence intensity in the absence and in the presence of a iridium complex (Q), K_{SV} is the Stern-Volmer quenching constant, K_q is the bimolecular quenching rate

constant, and τ_0 is in the absence of any quenching. The average life expectancy value of BSA in the case of agent is 10^{-8} seconds.[8] Using the Stern-Volmer equation, the K_q value is calculated to be 3.42×10^{13} $M^{-1}S^{-1}$, which is about 3 orders of magnitude higher than the pure dynamic quenching mechanism (2.0×10^{10} M^{-1} s^{-1}).[9] Therefore, the value of K_q indicates that the interaction between the iridium complex and BSA is dominated by the static quenching mechanism (Figure S4). The binding constant K_b and the number of complexes bound to BSA (n) can be calculated by the following equation (Equ 2).

$$\log\,[(F_0 - F)/F] = \log K_b + n \log [Q] \quad (2)$$

By calculation, the K_b and K_q values of complex **1** were $3.71x10^5$ M^{-1} and 3.42×10^{13} $M^{-1}S^{-1}$, respectively, indicating that the iridium complex has moderate binding ability to BSA. In addition, the study of BSA by synchronous fluorescence spectroscopy studied the molecular environment near the fluorophore.[10] The characteristic information of the tyrosine residue of BSA is $\Delta\lambda$ = 15 nm in the wavelength interval and the characteristic information of tryptophan residues is in the wavelength interval $\Delta\lambda$ = 60 nm. The fluorescence spectrum is shown in Figure 3. As the concentration of complex **1** increases, the intensity of fluorescence gradually decreases, and at $\Delta\lambda$ = 60 nm, a red shift from 286 nm to 287 nm occurs at the emission wavelength. The results indicate that complex **1** interacts with BSA efficiently by affecting the tryptophan microenvironment. The specific steps for the study of complex **2** and BSA are in the supporting information (Figures S2 – S4). Complex **2** is stronger than the interaction of complex **2** with BSA, which may be related to the cytotoxicity and structure of complex **2**. By studying the interaction between the complex and BSA, it was shown that the synthesized drug can be carried to the needed place by binding to BSA, and further affect the apoptosis of cancer cells (Table 2).

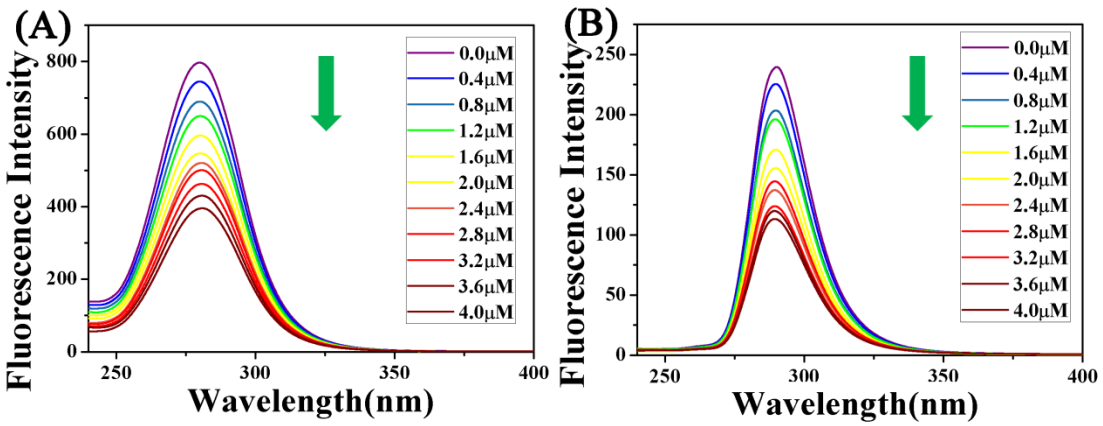

Figure S3. (A) Synchronous fluorescence spectrum of the reaction of BSA (10 μM, 50 mM Tris-HCl, 50 mM NaCl, pH = 7.2) with the complex **2** (0 ~4.0 μM) when Δλ = 60 nm, (B) Synchronous fluorescence spectrum of the reaction of BSA (10 μM, 50 mM Tris-HCl, 50 mM NaCl, pH = 7.2) with the complex **2** (0 ~4.0 μM) at Δλ = 15 nm. Arrows indicate changes in wavelength as the compound increases.

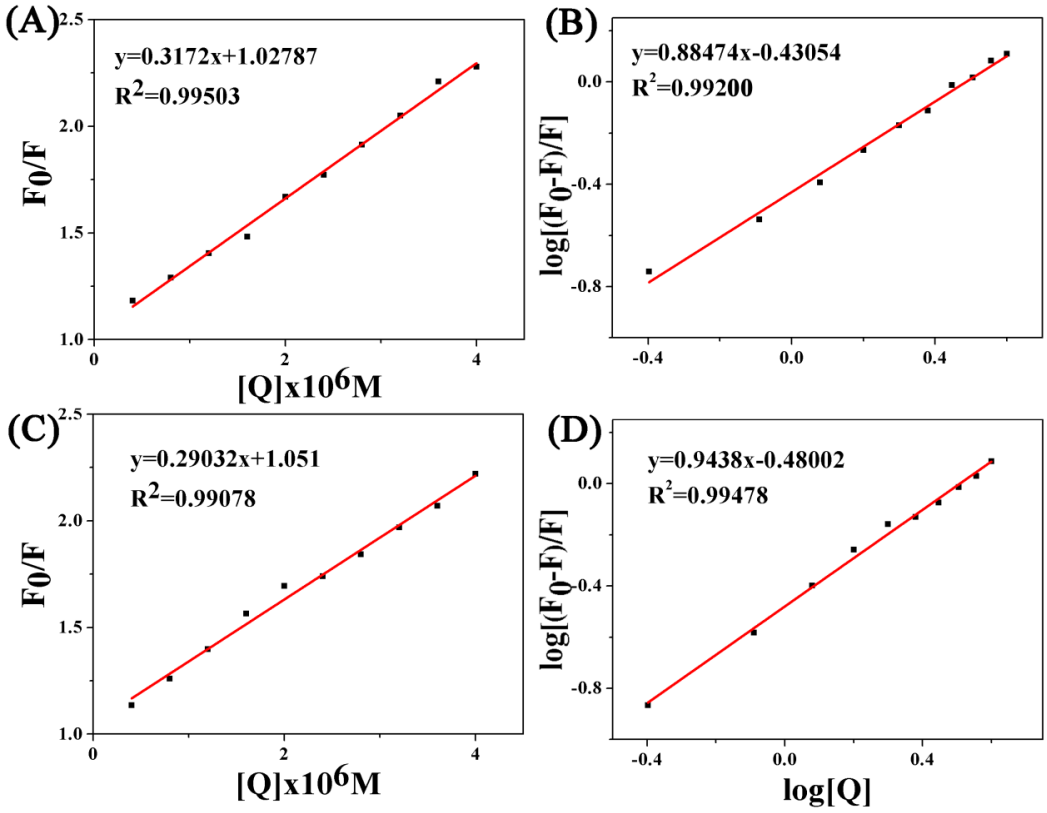

Figure S4 A) C) Stern–Volmer plots of F_0/F against the concentration of complexes **1** and **2**; **B) D)** Plots of $\log[(F_0 - F)/F]$ vs. log[Q] for the interaction of BSA with complexes **1** and **2**.

Cell Culture

Hela human cervical cancer cells and A549 human lung cancer cells were obtained from Shanghai Institute of Biochemistry and Cell Biology (SIBCB) and were grown in Dubelco's Modified Eagle Medium (DMEM). All media were supplemented with 10% fetal bovine serum, and 1 % penicillin-streptomycin solution. All cells were grown at 310 K in a humidified incubator under a 5 % CO_2 atmosphere.

Viability assay (MTT assay)

After plating 5000 A549 cells per well in 96-well plates, the cells were preincubated in drug-free media at 310 K for 24 h before adding different concentrations of the compounds to be tested. In order to prepare the stock solution of the drug, the solid complex was dissolved in DMSO. This stock was further diluted using cell culture medium until working concentrations were achieved. The drug exposure period was 24 h. Subsequently, 15 µl of 5 mg mL^{-1} MTT solution was added to form a purple formazan. Afterwards, 100 µl of dimethyl sulfoxide (DMSO) was transferred into each well to dissolve the purple formazan, and results were measured using a microplate reader (DNM-9606, Perlong Medical, Beijing, China) at an absorbance of 570 nm. Each well was triplicated and each experiment repeated at least three times. IC_{50} values quoted are mean ± SEM. The complex was serially diluted in DMSO prior to bioassay. The maximum working concentration of serially diluted DMSO was 1% (v / v), so the 1% DMSO itself does not cause cell growth inhibition in all of the bioassays.

Cell Cycle Analysis

A549 cells at 1.5×10^6 per well were seeded in a six-well plate. Cells were preincubated in drug-free media at 310 K for 24 h, after which drugs were added at concentrations of $0.25 \times IC_{50}$, $0.5 \times IC_{50}$, $1 \times IC_{50}$ and $2 \times IC_{50}$. After 24 h of drug exposure, supernatants were removed by suction and cells were washed with PBS. Finally, cells were harvested using trypsin-EDTA and fixed for 24 h using cold 70 % ethanol. DNA staining was achieved by resuspending the cell pellets in PBS containing propidium iodide (PI) and RNAse. Cell pellets were washed and resuspended in PBS before being analyzed in a flow cytometer (ACEA NovoCyte, Hangzhou, China) using excitation of DNA-bound PI at 488 nm, with emission at 585 nm. Data were

processed using NovoExpress™ software. The cell cycle distribution is shown as the percentage of cells containing G_0/G_1, S and G_2/M DNA as identified by propidium iodide staining. A549 cells were treated with complex 1 at the IC_{50} concentration of 0.25, 0.5, 1.0 and 2.0 for 24 hours (Figure 4, Tables S1)

Table S1. Cell cycle analysis carried out by flow cytometry using PI staining after exposing A549 cells to complex **1**.

		Population（%）		
Complex	**Ir concentrion**	**G_0/G_1 phase**	**S phase**	**G_2/M phase**
Control		60.92±1.40	25.02±0.42	11.97±0.54
	0.25×IC_{50}	54.85±2.01	30.07±0.20	13.15±0.23
	0.5×IC_{50}	53.69±0.51	30.19±0.12	12.91±0.01
Complex 1	1×IC_{50}	50.78±0.29	31.27±0.39	13.65±0.13
	2×IC_{50}	51.53±0.28	33.60±0.23	11.18±1.30

Induction of Apoptosis

Flow cytometry analysis of apoptotic populations of A549 cells caused by exposure to iridium complexes was carried out using the Annexin V-FITC Apoptosis Detection Kit (Beyotime Institute of Biotechnology, China) according to the supplier's instructions. Briefly, A549 cells (1.5×10^6 /2 mL per well) were seeded in a six-well plate. Cells were preincubated in drug-free media at 310 K for 24 h, after which drugs were added at concentrations of 0.25 × IC_{50}, 1 × IC_{50}, 2 × IC_{50} and 3 × IC_{50}. After 24 h of drug exposure, cells were collected, washed once with PBS, and resuspended in 195 μl of annexin V-FITC binding buffer which was then added to 5 μl of annexin V-FITC and 10 μL of PI, and then incubated at room temperature in the dark for 15 min. Subsequently, the buffer placed in an ice bath in the dark. The samples were analyzed by a flow cytometer (ACEA NovoCyte, Hangzhou, China). We tried to use the annexin V/PI method to

study whether complex **1** causes apoptosis (Table S2).

Table S2. Flow cytometry analysis to determine the percentages of apoptotic cells, using Annexin V-FITC vs S19 PI staining, after exposing A549 ells to complex **1**.

		Population (%)			
Complex	**Ir concentration**	**Viable**	**Early apoptosis**	**Late apoptosis**	**Non-viable**
control		93.11±0.9	0.90±0.18	5.44±0.26	0.55±0.03
Complex 1	0.5× IC_{50}	86.41±0.12	2.46±0.12	10.85±0.27	0.29±0.14
	1.0 × IC_{50}	61.88±0.2	6.57±0.50	27.58±0.21	3.97±0.38
	2.0 × IC_{50}	4.96±0.13	5.48±0.62	88.75±0.12	0.81±0.14
	3.0 × IC_{50}	2.59±0.29	10.99±0.13	85.72±0.54	0.70±0.17

Cellular localization assay

Two Photon Laser Scanning Microscope (*/LSM/880NLO) is produced at Carl Zeiss AG, Germany. LTDR (Life Technologies, USA), MTDR (Life Technologies, USA), CCCP (Sigma Aldrich, USA), chloroquine (Sigma Aldrich, USA) were used as received.

A549 cells were seeded into 35 mm dishes (Greiner, Germany) for confocal microscopy. After cultured overnight, the cells were incubated with complexes **1, 2** at 1×IC_{50} for 1 h. The treated cells were observed immediately under a confocal microscope with excitation at 488 nm. For colocalization studies, the cells were incubated with complexes (1×IC_{50}) for 1 h. Subsequently, the medium was replaced with staining medium containing MTDR/LTDR (500 nM) and stained

for another 30 min and 1 h (Figure S5). The cells were washed twice with PBS, and then viewed immediately under a confocal microscope.

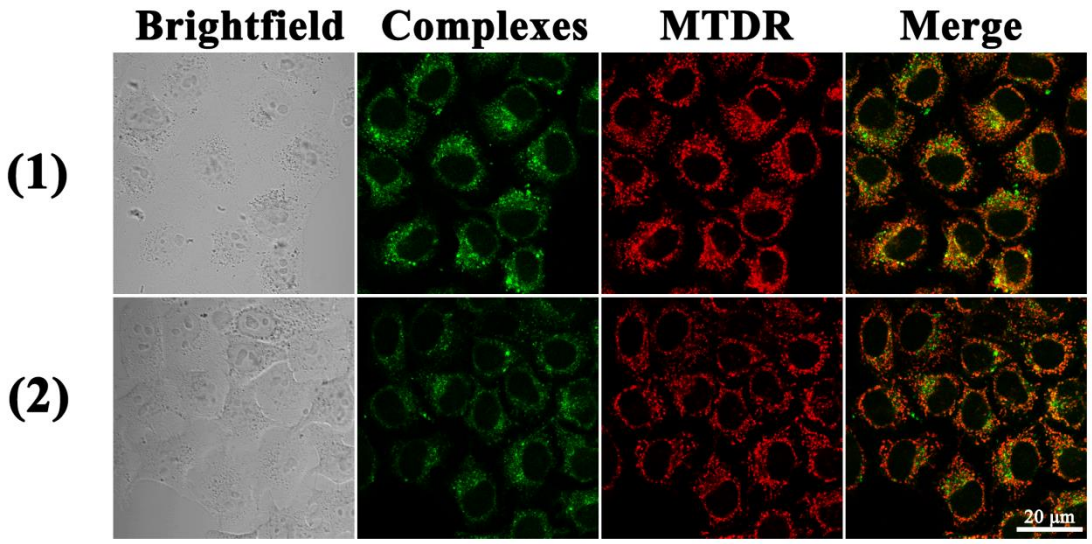

Figure S5 Intercellular colocalisation of complexes **1** and **2** with MTDR. A549 cells were incubated with $1\times IC_{50}$ of complexes **1** and **2** and at 1 h, then stained with MTDR (500 nM, 1 h) at 310 K. Complexes **1** and **2**: λex = 488 nm and λem = 500-600 nm; MTDR, λex = 644 nm and λem = 660-720 nm). Scale bar: 20 μm.

First, we selected complex **1** to study how the complexes entered the cells, pre-treating A549 cells at 310 K and 277 K, respectively. In addition, A549 cells were pretreated with carbonylcyanide m-chlorophenylhydrazone (CCCP, metabolic inhibitor 50 μM) and chloroquine (endocytosis modulator 50 μM), and laser confocal contrast experiments were performed on the samples under the same parameters. The experimental results show that at room temperature (310 K), complex **1** ($1\times IC_{50}$) mainly enter the cell cytoplasm, but at 277 K and CCCP-treated A549 cells. As a result, the efficiency of cell entry was significantly reduced, but treatment of A549 cells with chloroquine was almost the same as at room temperature. This shows that iridium complexes and ruthenium complexes in this system mainly enter into the cells in an energy-dependent manner.Investigation of drug entry pattern: Cells were incubated with complex ($1\times IC_{50}$) for 1 h, after which media was replaced with staining medium containing CCCP (50 μM, 10 min) chloroquine (50 μM, 10 min) and re-stained for 15 min. The cells were washed twice with PBS, and then viewed immediately under a confocal

microscope.

Mitochondrial Membrane Assay

Analysis of the changes of mitochondrial potential in cells after exposure to iridium complexes was carried out using the mitochondrial membrane potential assay kit with JC-1 (Beyotime Institute of Biotechnology, Shanghai, China) according to the manufacturer's instructions. Briefly, 1.5×10^6 A549 cancer cells were seeded in six-well plates left to incubate for 24 h in drug-free medium at 310 K in a humidified atmosphere. Drug solutions, at concentrations of $0.25 \times IC_{50}$, $0.5 \times IC_{50}$, $1.0 \times IC_{50}$ and $2.0 \times IC_{50}$ of complex **1** against A549 cancer cells, were added in triplicate, and the cells were left to incubate for a further 24 h under similar conditions (Figure S6 and Table S3). Supernatants were removed by suction, and each well was washed with PBS before detaching the cells using trypsin-EDTA. Staining of the samples was done in flow cytometry tubes protected from light, incubating for 30 min at ambient temperature. The samples were immediately analyzed by a flow cytometer (ACEA NovoCyte, Hangzhou, China). For positive controls, the cells were exposed to carbonyl cyanide 3-chlorophenylhydrazone, CCCP (5 μM) for 10 min. Data were processed using Novo Express™ software.

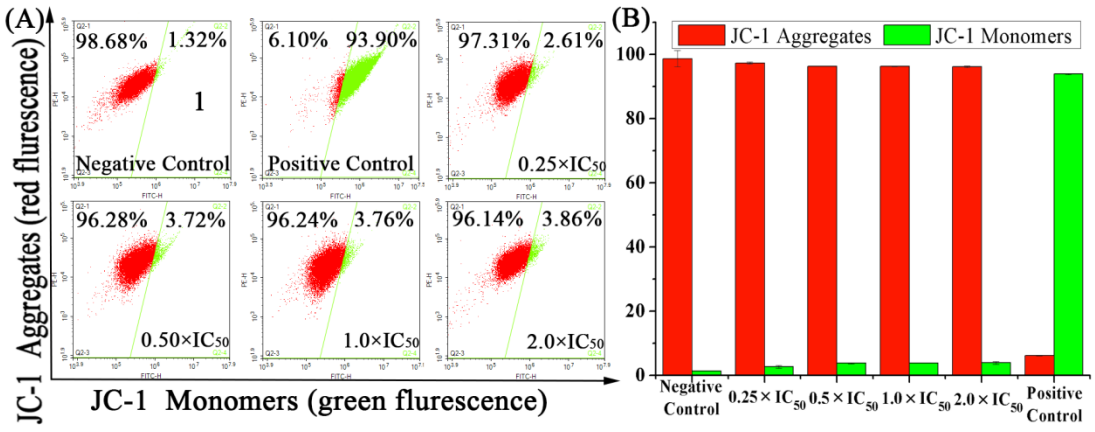

Figure S6. (A) Effects of complex **1** on MMP analyzed by JC-1 staining and flow cytometry. A549 cells were

treated with vehicle or complexes at the indicated concentrations for 24 h.(B) Histogram of changes in mitochondrial membrane potential in A549 cells treated with complex **1**. Data reference is the mean of three replicate ± SD.

Table S3. The mitochondrial membrane polarization of A549 cells induced by complex **1**.

		Population（%）	
complex	**Ir Concentration**	**JC-1 Aggregates**	**JC-1 Monomers**
	$0.25\times IC_{50}$	97.31±0.28	2.61±0.42
	$0.5\times IC_{50}$	97.31±0.28	2.61±0.42
	$1.0\times IC_{50}$	96.24±0.6	3.76±0.4
complex 1	$2.0\times IC_{50}$	96.14±0.27	3.86±0.27
Negative control		98.68±2.54	1.32±0.04
Positive conctrol		6.10±0.13	93.90±0.15

ROS Determination

Flow cytometry analysis of ROS generation in A549 cells caused by exposure to iridium complex was carried out using the Reactive Oxygen Species Assay Kit (Beyotime Institute of Biotechnology, Shanghai, China) according to the supplier's instructions. Briefly, 1.5×10^6 A549 cells per well were seeded in a six-well plate. Cells were preincubated in drug-free media at 310 K for 24 h in a 5 % CO_2 humidified atmosphere, and then drugs were added at concentrations of 0.25

× IC_{50} and 0.5 × IC_{50}. After 24 h of drug exposure, cells were washed twice with PBS and then incubated with the DCFH-DA probe (10 μM) at 310 K for 30 min, and then washed triple immediately with PBS. The fluorescence intensity was analyzed by flow cytometry (ACEA NovoCyte, Hangzhou, China). Data were processed using Novo Express™ software. At all times, samples were kept under dark conditions to avoid light-induced ROS production. Therefore, we used flow cytometry to detect the amount of NF-κBp65 protein in the cells exposed to the complex **1**(Figure S7).

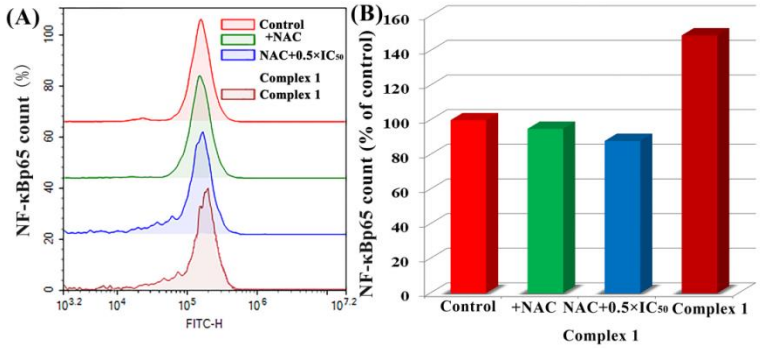

Figure S7. (A) Effect of complex **1** on intracellular NF-κBp65 protein content in A549 lung cancer cells treated at the indicated concentrations for 24 h. (NAC concentration：10 mM) (B) The histogram shows the NF-κBp65 protein content induction in A549 cancer cells treated with complex **1** (NAC concentration：10 mM).

Reaction with NADH

The reaction of complexes **1** and **2** (ca. 1 μM) with NADH (ca. 100 μM) in 20%MeOH/80% H_2O (v/v) was monitored by UV-Vis at 298 K after various time intervals. TON was calculated from the difference in NADH concentration after 8 h divided by the concentration of iridium catalyst. The concentration of NADH was obtained using the extinction coefficient ε_{339} = 6220 $M^{-1}cm^{-1}$. We investigated the reaction of complexes **1** and **2** (1 μM) with NADH (100 μM) in 20% MeOH / 80% H2O (v / v) by UV-vis at 298K for 8 hours (Figure S8).

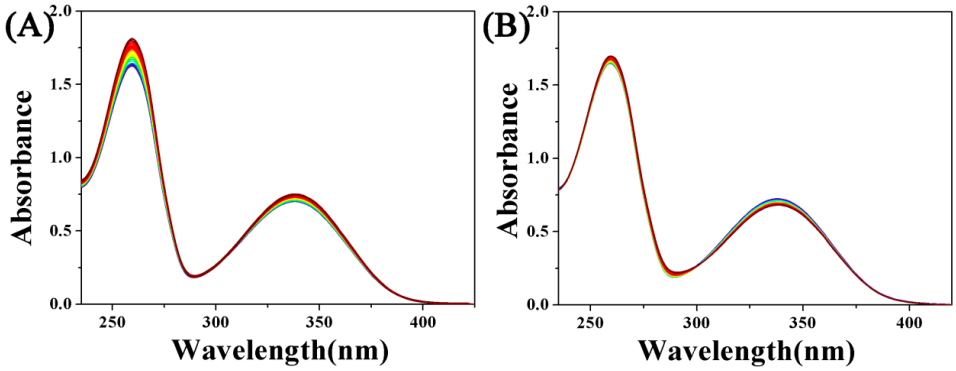

Figure S8. (A) UV-Vis spectra of the reaction of NADH (100 μM) with complex **1** (1 μM) and (B) complex **2** (1 μM) in 20% MeOH/80%H_2O (v/v) at 298 K for 8 h.

Transwell Migration Assay

Transwell migration assays were performed by using transwell chamber in 24-well cell culture plate with 8 μm pores. Chambers were washed with PBS for three times. Then the 600 μl medium with the tested compounds at concentration of IC_{50} was placed in the lower chamber, and A549 cancer cells (2×10^5/well) in 200 μl serum-free medium were seeded in the top chamber. After incubation for 24 h, non-migrated cells on the top surface of the membrane were gently scraped away with cotton swab, and migrated cells were fixed with 4% paraformaldehyde for 20 min and stained with 0.1% crystal violet for 30 min. The cells that migrated to the lower side of the membranes were imaged and counted using a microscope. In order to further prove that the complex has the antimetastatic ability of cancer cells, we used flow cytometry to detect the content of MMP-9 in the cells exposed to the complex (Figure S9)

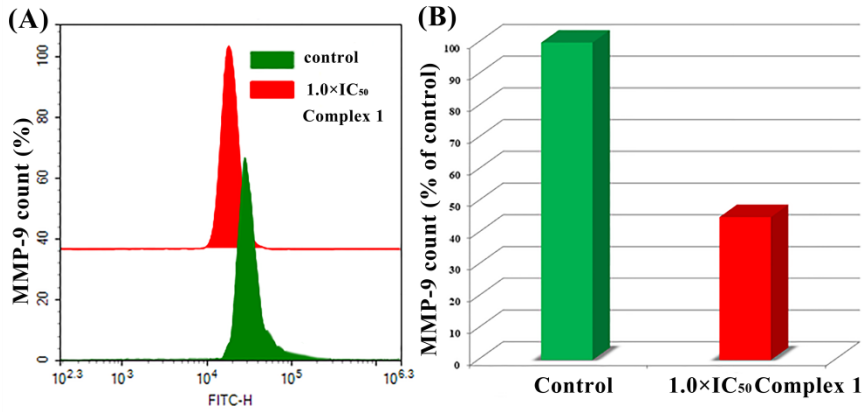

Figure S9. (A) Effect of complex **1** on intracellular MMP-9 content in A549 lung cancer cells treated at the indicated concentrations for 24 h. (B) The histogram shows the MMP-9 content induction in A549 cancer cells treated with complex **1**.

Acridine Orange assay

A549 cells seeded into six-well plate (Corning) were exposed to complex **1** at theindicated concentrations for 12 h. The cells were then washed twice with FBS annd incubated with AO (5 μM) at 310 K for 15 min. The cells were washed twice with PBS and visualized by confocal microscopy (LSM/880NLO). Emission was colleted at 510 ± 20 nm (green) and 625 ± 20 nm (red) upon excitation at 488 nm.

Materials and Syntheses

$IrCl_3 \cdot nH_2O$, 2,3,4,5-tetramethyl-2-cyclopentenone (95%), Butyllithium solution (1.6 M in hexane), rhodamine B, rhodamine 6G, hydrazine hydrate, 4-(2-pyridyl)-benzaldehyde purchased from Sigma-Aldrich. Dimer and ligands L_1 ~ L_2 were prepared as described. For biological experiments, BSA, DMEM medium, fetal bovine serum, penicillin / streptomycin mixture, trypsin / EDTA, cisplatin, MTT and phosphate buffered saline (PBS) were purchased from Sangon Biotech. Stock solutions of cisplatin (10 mM) and complexes **1** ~ **2** (10 mM) were prepared in DMSO. Test compounds were dissolved in DMSO, stock solutions stored at -20 °C, thawed prior to use and diluted with medium. ^{1}H NMR spectra were acquired in 5 mm NMR tubes at 298 K on Bruker DPX 500 (^{1}H = 500.13 MHz) spectrometers. ^{1}H NMR chemical shifts were internally referenced to $(CHD_2)(CD_3)SO$ (2.50 ppm) for DMSO-d_6, $CHCl_3$ (7.26 ppm) for chloroform-d_1. All data processing was carried out using XWINNMR

version 3.6 (Bruker UK Ltd).

Rhodamine B hydrazide was synthesized by a one-step reaction of rhodamine B with hydrazine hydrate in ethanol. To a 100 mL round bottom flask was added rhodamine B, 30 mL absolute ethanol was added, stirred rapidly at room temperature, an excessive hydrazine hydrate (8 mL)was added, the mixture was stirred under reflux until pink color to orange color and yellow precipitate precipitated, then, The reaction was cooled to room temperature, 1 M HCl was added and the solution turned to blood red. The pH of the solution was adjusted to 9-10 with 1 M NaOH. The color of the solution changed to an orange-yellow color and a white precipitate was formed. The precipitate was filtered, washed with water (3×25 mL) and dried to give a white solid , the solid was dissolved in water and extracted with dichloromethane (3×25 mL) to remove excessive hydrazine hydrate, organic layer was dried to give a purple-white solid. Rhodamine 6G hydrazide : The procedure was similar to that described for the synthesis of rhodamine B hydrazide. Reactant: rhodamine 6G (4.80 g,10 mmol) with hydrazine hydrate (8 mL).

Rhodamine 6G hydrazide: Yield: 2.48g (58%). ^{1}H NMR (500 MHz, $CDCl_3$) δ 7.98 – 7.94 (m, 1H), 7.49 – 7.44 (m, 2H), 7.07 – 7.04 (m, 1H), 6.43 (dd, *J* = 45.7, 17.8 Hz, 2H), 6.28 (s, 2H), 3.62 (s, 2H), 3.24 (dd, *J* = 13.9, 6.9 Hz, 4H), 1.96 (s, 6H), 1.34 (t, *J* = 7.0 Hz, 6H).

Rhodamine B hydrazid: Yield: 2.82g (62%). ^{1}H NMR (500 MHz, $CDCl_3$) δ 7.97 – 7.93 (m, 1H), 7.47 (d, *J* = 1.8 Hz, 2H), 7.10 (dd, *J* = 5.7, 2.7 Hz, 1H), 6.57 – 6.24 (m, 6H), 3.72 – 3.59 (m, 2H), 3.34 (d, *J* = 3.7 Hz, 8H), 1.18 (s, 12H).

L_1-L_2：To a 0.856g (2 mmol) of rhodamine 6G hydrazide(rhodamine B hydrazide) dissolved in 30 mL of dichloromethane ,a 0.364 g (2 mmol) 4-(2-pyridyl)-benzaldehyde was added, a drop of formic acid was added dropwise and heated to reflux for 24 h. The mixture was cooled to room temperature, the solvent was evaporated to dryness on a rotary evaporator to afford purple oil. Add a small amount of methanol dropwise to precipitate a white solid which was then filtered and washed with methanol.

Complexes **1 - 2** was obtained by the reaction of L_1-L_2 (0.10 mmol) with $[(\eta^5\text{-}Cp^x)IrCl_2]_2$ and 10 equivalents of sodium acetate, in a solventmixture (30 mL) of CH_2Cl_2 and MeOH (1:1 v/v)

under reflux condition for 12 h. The solution turned blood red, after a period of time, a red residue appears, spin the solution, dissolved in hot methanol and precipitated the red solid the precipitate was orange red. The precipitate was dissolved in methylene chloride, filtered through celite, spin the liquid, dissolved with as little methylene chloride as possible, and recrystallized by adding ether. The product was orange-red crystals.

^{1}H NMR spectra were acquired in 5 mm NMR tubes at 298 K on Bruker DPX 500 (^{1}H= 500.13 MHz) spectrometers. ^{1}H NMR chemical shifts were internally referenced to $(CHD_2)(CD_3)SO$ (2.50ppm) for DMSO-d_6, $CHCl_3$ (7.26 ppm) for chloroform-d_1. All data processing was carried out using XWINNMRversion 3.6 (Bruker UK Ltd.).

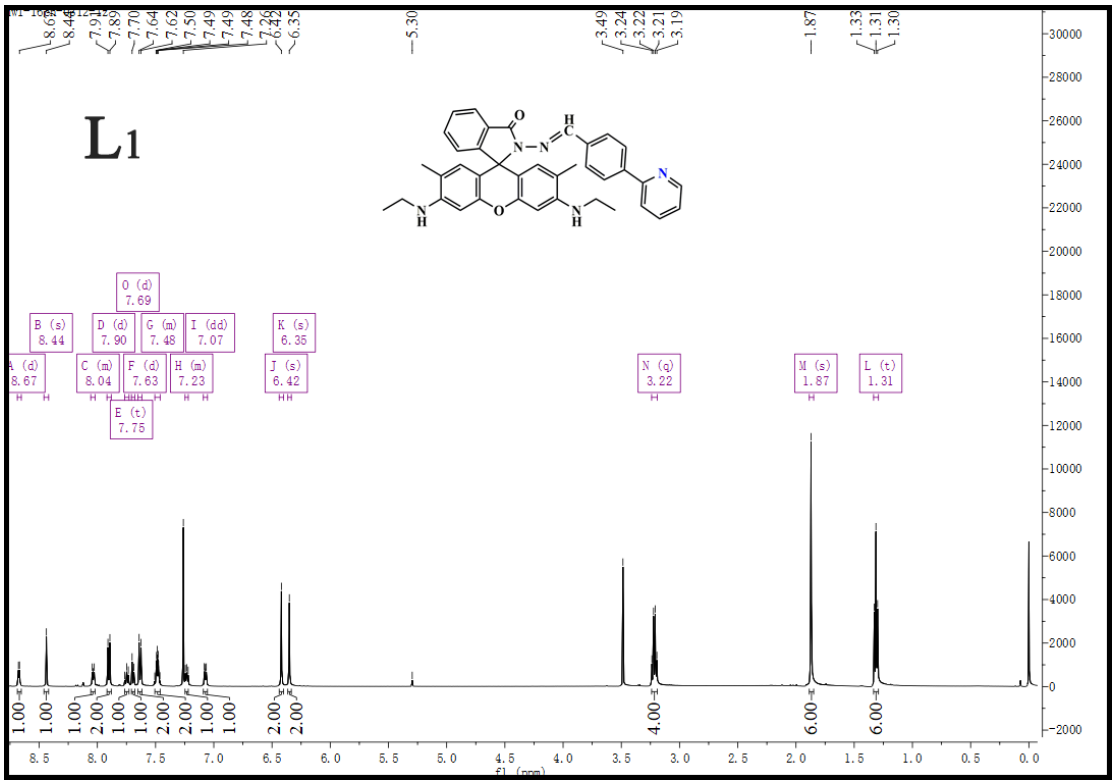

Figure S10. The ^{1}H NMR (500.13 MHz, $CDCl_3$) peak integrals of L_1.

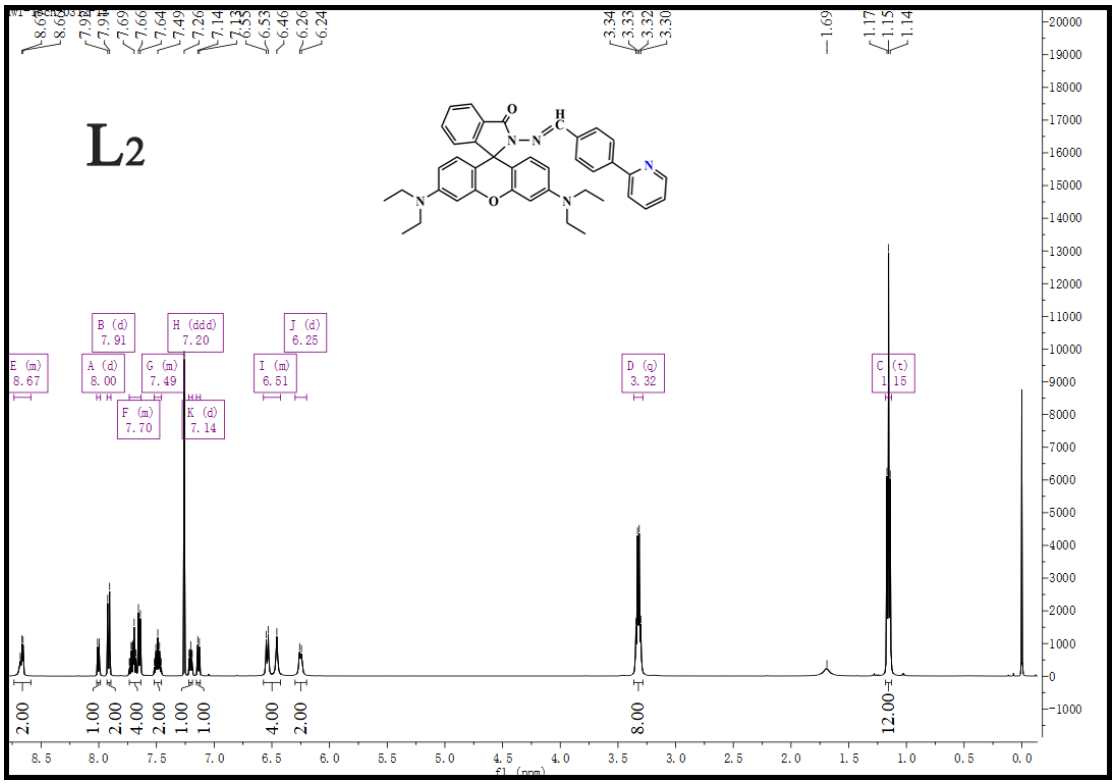

Figure S11. The ^{1}H NMR (500.13 MHz, $CDCl_3$) peak integrals of L_2.

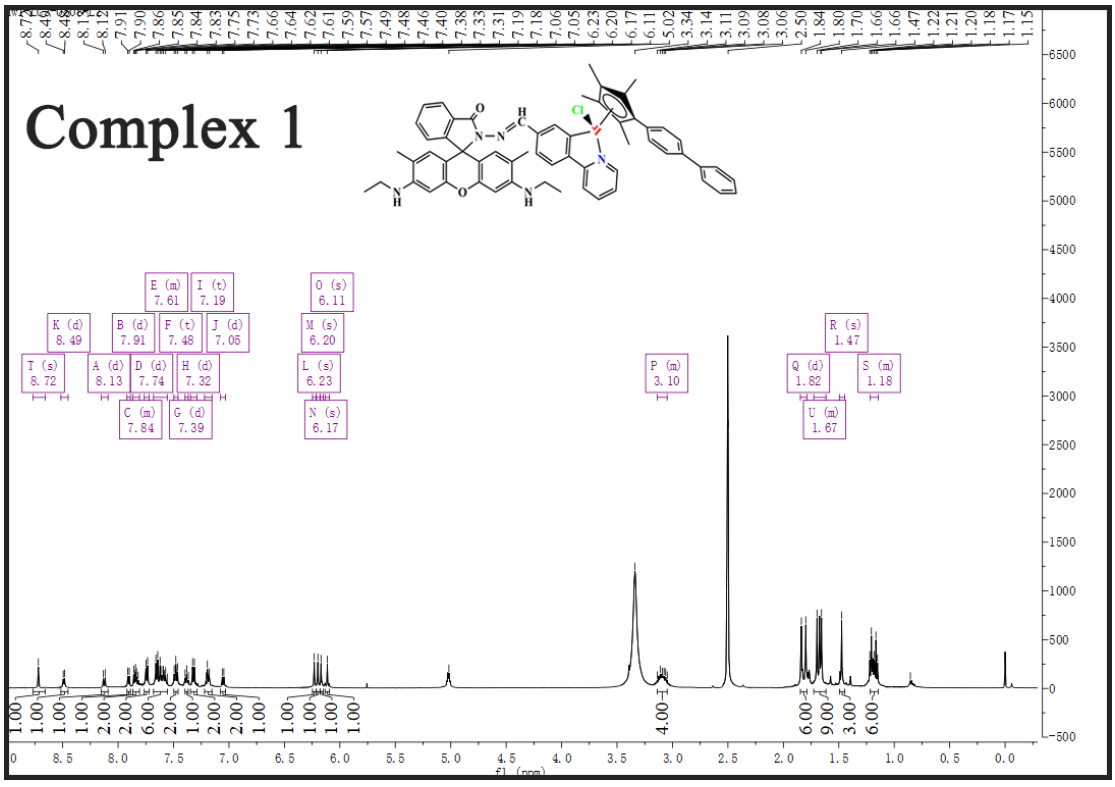

Figure S12. The ^{1}H NMR (500.13 MHz, DMSO) peak integrals of $[(\eta^5\text{-}C_5Me_4C_6H_4C_6H_5)Ir(L_1)Cl]PF_6$ (complex

1).

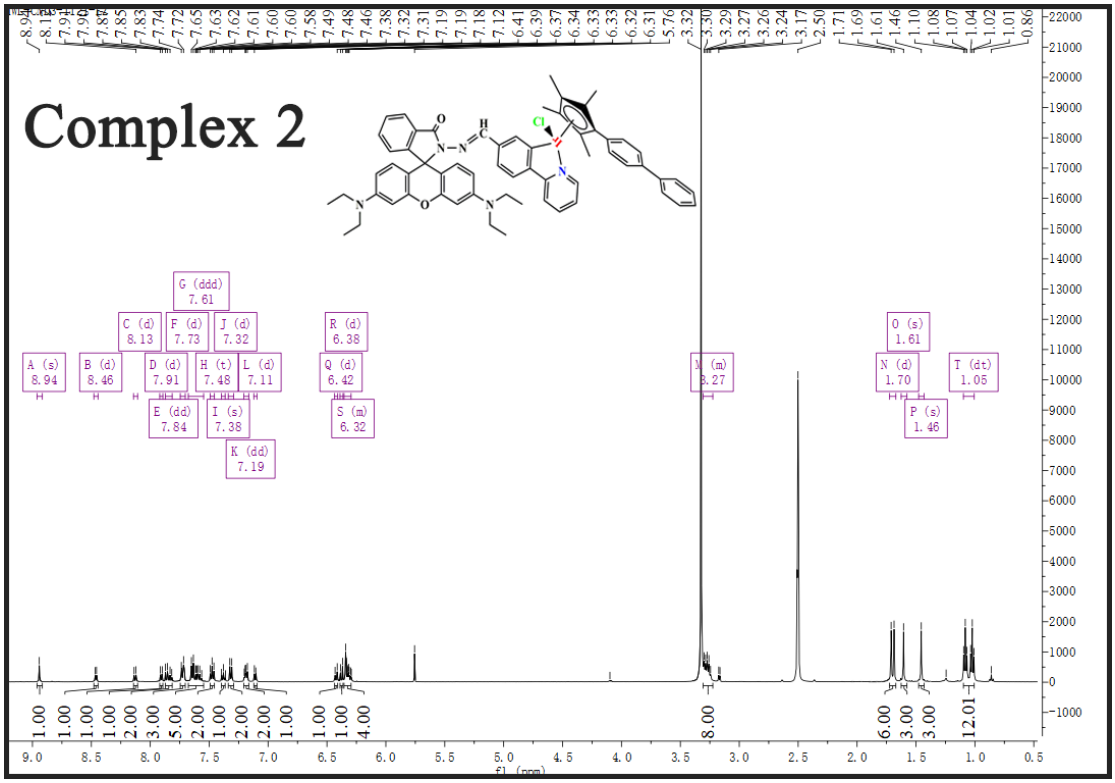

Figure S13. The ^{1}H NMR (500.13 MHz, DMSO) peak integrals of $[(\eta^5\text{-}C_5Me_4C_6H_4C_6H_5)Ir(L_2)Cl]PF_6$ (complex **2**).

MS was measured on a LCQ Advantage MAX mass spectrometer. Elemental analysis was performed on a VarioMICRO CHNOS elemental analyzer. UV/Vis spectroscopy was performed on a TU-1901 UV spectrometer. The fluorescence spectra were collected by a fluorescence spectrophotometer (F-4600, Hitachi) with a 400 V voltage and 5 nm slit width for both excitation and emission.

Complex **1**: MS: m/z：1058.92.$[(\eta^5\text{-}C_5Me_4C_6H_4C_6H_5)Ir(L_1)]^+$.

Complex **2**: MS: m/z：1086.05.$[(\eta^5\text{-}C_5Me_4C_6H_4C_6H_5)Ir(L_2)]^+$.

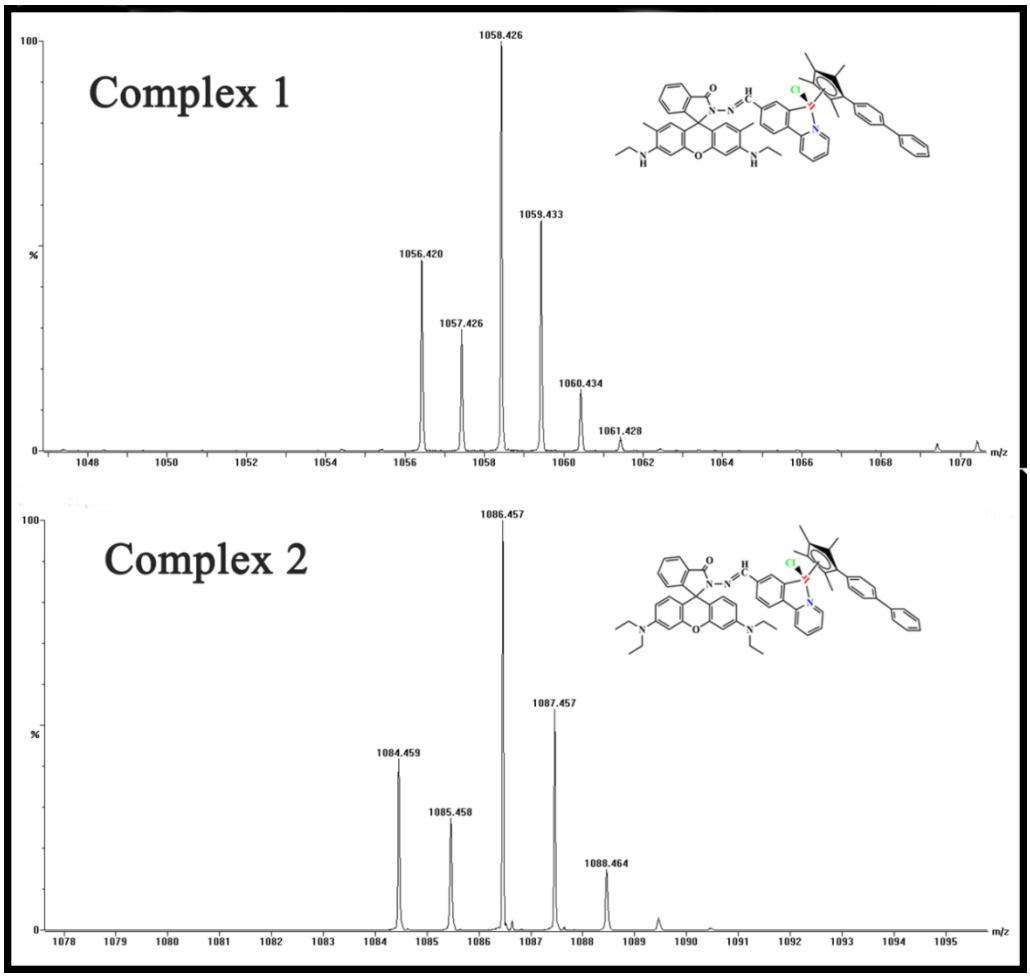

Figure S14. The mass spectrometry of complexes **1** ~ **2**.

References

(1) Birchard, K., A spectroscopic investigation on the interaction of a magnetic ferrofluid with a model plasma protein: effect on the conformation and activity of the protein. *Phy. Chem. Chem. Phy.* **2012,** *14*, 15482-15493.

(2) Samari, F.; Hemmateenejad, B.; Shamsipur, M.; Rashidi, M.; Samouei, H., Affinity of Two Novel Five-Coordinated Anticancer Pt(II) Complexes to Human and Bovine Serum Albumins: A Spectroscopic Approach. *Inorg. Chem.* **2012,** *51*, 3454-3464.

(3) Shahabadi, N.; Kashanian, S.; Darabi, F., DNA binding and DNA cleavage studies of a water soluble cobalt(II) complex containing dinitrogen Schiff base ligand: the effect of metal on the mode

of binding. *Eur. J. Med.Chem.* **2010,** *45*, 4239-4245.

(4) Tabassum, S.; Singh, R.; Zaki, M.; Ahmad, M.; Afzal, M., Synthesis and crystal structure determination of a mononuclear cobalt(II) complex derived from 4-(pyridin-4-ylmethoxy)-benzoic acid: evaluation of the DNA/protein interaction and photo-induced pBR322 DNA cleavage. *Rsc. Adv.* **2015,** *5*, 35843-35851.

(5) Li, D.; Zhu, M.; Xu, C.; Ji, B., Characterization of the baicalein-bovine serum albumin complex without or with Cu2+ or Fe3+ by spectroscopic approaches. *Eur. J. Med. Chem.* **2011,** *46*, 588-599.

(6) Zhu, J.; Wu, L.; Zhang, Q.; Chen, X.; Liu, X., Investigation the interaction of Daphnin with human serum albumin using optical spectroscopy and molecular modeling methods. *Spectrochim. Acta. A.* **2012,** *95*, 252-257.

(7) Pettinari, R.; Marchetti, F.; Petrini, A.; Pettinari, C.; Lupidi, G.; Fernández, B.; Diéguez, A. R.; Santoni, G.; Nabissi, M., Ruthenium(II)-arene complexes with dibenzoylmethane induce apoptotic cell death in multiple myeloma cell lines. *Inorg. Chim. Acta.* **2017,** *454*, 139-148.

(8) Chatterjee, S.; Mukherjee, T. K., Spectroscopic investigation of interaction between bovine serum albumin and amine-functionalized silicon quantum dots. *Phy. Chem. Chem. Phy.* **2014,** *16*, 8400-8.

(9) Zhang, Y. Z.; Zhou, B.; Liu, Y. X.; Zhou, C. X.; Ding, X. L.; Liu, Y., Fluorescence Study on the Interaction of Bovine Serum Albumin with P-Aminoazobenzene. *J. Fluoresc.* **2008,** *18*, 109-118.

(10) Tang, J.; Luan, F.; Chen, X., Binding analysis of glycyrrhetinic acid to human serum albumin: fluorescence spectroscopy, FTIR, and molecular modeling. *Bioorgan. Med. Chem.* **2006,** *14*, 3210-3217.